International Journal of Wavelets, Multiresolution
and Information Processing
Vol. 3, No. 1 (2005) 19–42

World Scientific
www.worldscientific.com

CONTINUOUS WAVELET TRANSFORM MODULUS MAXIMA ANALYSIS OF THE ELECTROCARDIOGRAM: BEAT CHARACTERISATION AND BEAT-TO-BEAT MEASUREMENT

I. ROMERO LEGARRETA*, P. S. ADDISON*,†, M. J. REED‡, N. GRUBB§,
G. R. CLEGG‡, C. E. ROBERTSON‡ and J. N. WATSON†

*Faculty of Engineering and Computing, Napier University, Merchiston Campus
10 Colinton Road, Edinburgh, EH10 5DT, UK

†Cardiodigital Ltd, Elvingston Science Centre, Gladsmuir, East Lothian, EH33 1EH, UK

‡Accident and Emergency Department, The Royal Infirmary of Edinburgh
15 Little France Crescent, Edinburgh, EH16 4SU, UK

§Department of Cardiology, The Royal Infirmary of Edinburgh
15 Little France Crescent, Edinburgh, EH16 4SU, UK

Received 9 December 2003

The problem of automatic beat recognition in the ECG is tackled using continuous wavelet transform modulus maxima (CWTMM). Features within a variety of ECG signals can be shown to correspond to various morphologies in the CWTMM domain. This domain has an easy interpretation and offers a useful tool for the automatic characterization of the different components observed in the ECG in health and disease. As an application of this enhanced time-frequency analysis technique for ECG signals, an *R*-wave detector is developed and tested using patient signals recorded in the Coronary Care Unit of the Royal Infirmary of Edinburgh (attaining a sensitivity of 99.53% and a positive predictive value of 99.73%) and with the MIT/BIH database (attaining a sensitivity of 99.70% and a positive predictive value of 99.68%).

Keywords: ECG analysis; beat detection; wavelet transform modulus maxima.

1. Introduction

The surface electrocardiogram (ECG) is a crucial diagnostic investigation in many areas of modern medicine. Analysis of the ECG has become an important area of research, in particular where advanced signal processing techniques can yield useful and timely information, which is otherwise inaccessible, e.g. the identification of ventricular fibrillation during cardiac resuscitation. Traditionally, analytical tools extracting time-frequency information have been based around the Fourier transform.[1,2] More recently, the Continuous Wavelet Transform (CWT) has been used successfully in the processing of ECG signals, and offers significant

advantages — in particular the preservation of location specific features.[3–5] In this paper we explore the use of CWT modulus maxima in the analysis of beat morphologies, and in particular the detection of individual beats in large data sets.

The paper is structured as follows: Sec. 2 covers the basic theory of the CWT and the derivation of its modulus maxima. Section 3 illustrates various beat morphologies as described using their modulus maxima. Section 4 briefly reviews current beat detection algorithms and describes the new automated beat detection algorithm proposed by the authors, which has the CWTMM at its core. Section 5 reports results from the testing of the new algorithm with *in-house* data collected from the Coronary Care Unit (CCU) at the Royal Infirmary of Edinburgh. The algorithm is then tested on the standard MIT/BIH database. The work is summarized in Sec. 6 and concluding remarks are made.

2. Background

Continuous Wavelet Transform (CWT) differs from the more traditional Short Time Fourier Transform (STFT) as it allows the arbitrarily high localisation in time, of high frequency signal features. The CWT does this by having a variable window width which is related to the scale of observation — a flexibility that allows for the isolation of the high frequency features. In effect, the Heisenberg boxes associated with the analysing wavelet function change shape in the time frequency plane becoming tall and thin at high frequencies and short and wide at lower frequencies, whereas the fixed window of the STFT dictates Heisenberg boxes of constant dimensions across the time-frequency plane. Another important distinction is that the CWT is not limited to using sinusoidal analysing functions, but rather can employ a large selection of localised waveforms as long as they satisfy predefined mathematical criteria.

In this section, a brief review of the CWT and its defining properties is presented. The modulus maxima of the transform surface in wavelet space are then defined. Finaly, the conversion from wavelet scale to wavelet frequency used in this paper is discussed.

2.1. *Wavelet transform*

The wavelet transform of a continuous time signal, $x(t)$, is defined as:

$$T(a,b) = \frac{1}{\sqrt{a}} \int_{-\infty}^{+\infty} x(t)\psi^*\left(\frac{t-b}{a}\right) dt, \tag{1}$$

where $\psi^*(t)$ is the complex conjugate of the wavelet function $\psi(t)$, a is the dilation parameter of the wavelet and b is the location parameter of the wavelet.

In order to be classified as a wavelet, a function must satisfy certain mathematical criteria.

These are:

(a) A wavelet must have finite energy: $E = \int_{-\infty}^{+\infty} |\psi(t)|^2 \, dt < \infty.$ (2)

(b) If $\hat{\phi}(f)$ is the Fourier transform of $\psi(t)$, i.e. $\hat{\psi}(\omega) = \int_{-\infty}^{\infty} \psi(t) e^{-i(\omega)t} \, dt,$ (3)

then the following condition must hold: $C_g = \int_0^{\infty} \frac{|\hat{\psi}(\omega)|^2}{\omega} \, d\omega < \infty.$ (4)

This implies that the wavelet has no zero frequency component. Equation (4) is known as the *admissibility condition* and C_g is called the *admissibility constant*. The value of C_g depends on the chosen wavelet.

(c) For complex (or analytic) wavelets, the Fourier transform must both be real and vanish for negative frequencies.

The contribution to the signal energy at the specific a scale and b location is given by the two-dimensional wavelet energy density function known as the scalogram:

$$E(a, b) = |T(a, b)|^2. \tag{5}$$

The contribution to the total energy distribution contained within the signal at a specific a scale is given by the integral of $E(a, b)$ with respect to b. Known as wavelet variance it may be used to find dominant scales associated with the signals and has been used often, for example, in the study of coherent structures found in turbulent fluid flows.[9–11] The total energy in the signal may be found from its wavelet transform as follows:

$$E = \frac{1}{C_g} \int_{-\infty}^{+\infty} \int_0^{\infty} \frac{1}{a^2} |T(a, b)|^2 \, da \, db \quad \left[= \int_{-\infty}^{+\infty} x(t)^2 \, dt \right]. \tag{6}$$

In practice a fine discretisation of the CWT is computed where the b location is usually discretised at the sampling interval and the a scale is discretised logarithmically. The a scale discretisation is often taken as integer powers of 2; however, when finer resolution is required (as it is in the methods presented herein) this may be changed to fractional powers of two.[12] The discretised CWT is made distinct from the discrete wavelet transform (DWT) in the literature. In its basic form, the DWT employs a dyadic grid (integer power of two scaling in a and b) and orthonormal wavelet basis functions and exhibits zero redundancy. (Actually, the transform integral remains continuous for the DWT but is determined only on a discretised grid of a scales and b locations. In practice, the input signal is treated as an initial wavelet approximation to the underlying continuous signal from which, using a multiresolution algorithm, the wavelet transform and inverse transform can be computed discretely, quickly and without loss of signal information.) Many variants of the DWT exist including most notably the stationary or Dyadic Wavelet

Transform (or DyWT), which allows a finer, more regular discretisation of the signal in time. Although this destroys orthogonality, it is useful for some statistical applications.[13] In this paper, however, we concern ourselves only with the CWT as it allows arbitrarily high resolution in the time-frequency plane allowing each modulus maxima line to be followed with certainty across scales.[14,15]

2.2. *Modulus maxima*

Wavelet *modulus maxima*, defined as:

$$\frac{d|T(a,b)|^2}{db} = 0 \tag{7}$$

are used for locating and characterising singularities in the signal (note that Eq. (7) also includes inflection points with zero gradient. These can be easily removed when implementing the modulus maxima method in practice). Modulus maxima-based methods are beginning to find favour in the analysis of a variety of signals including in engineering and medical signals, and the characterisation of multifractal signals.[8,16–25]

In this study we employ the Mexican hat wavelet, which is the second derivative of a Gaussian function, defined as:

$$\psi(t) = (1 - t^2)e^{\frac{t^2}{2}} \tag{8}$$

and shown in Fig. 1 This wavelet has been used in practice for a number of data analysis tasks in engineering, including the morphological characterisation of engineering surfaces, the interrogation of laser-induced ultrasonic signals and the analysis of turbulent flows.[15] The Mexican hat is used extensively in studies requiring the use of modulus maxima methods as its maxima lines (and those of other derivatives of Gaussian functions) are guaranteed continuous across scales for singularities in the signal.[26]

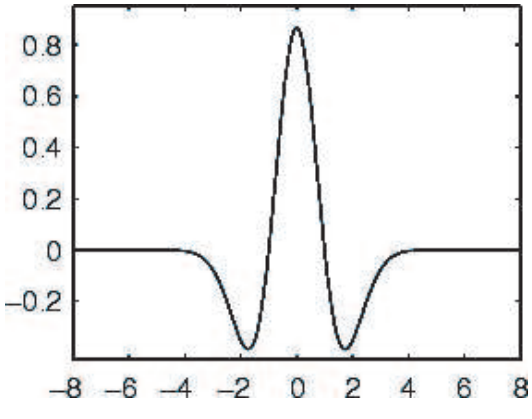

Fig. 1. The second derivative of a Gaussian function: the Mexican hat.

2.3. *Conversion from wavelet scale to frequency*

In this paper we use the conversion from wavelet scale to wavelet frequency given by the following expression:

$$f = \frac{f_c}{a \cdot \Delta t} \tag{9}$$

where:

a is the wavelet scale,
f_c is a characteristic frequency of the wavelet,
Δt is the sampling period, $(\Delta t = 1/f_s)$.

In the case of the Mexican hat wavelet, the characteristic frequency we employ is the standard deviation of the power spectrum,[14] i.e. $f_c = \left(\sqrt{5/2}\right)/2\pi = 0.251$.

3. Modulus Maxima in the Analysis of ECG Signals: Beat Morphologies

This section considers the analysis of different shapes of QRS complexes from both healthy and diseased hearts using the Mexican hat-based CWT. Figure 2 contains four typical QRS signals with their respective wavelet transforms plotted below.

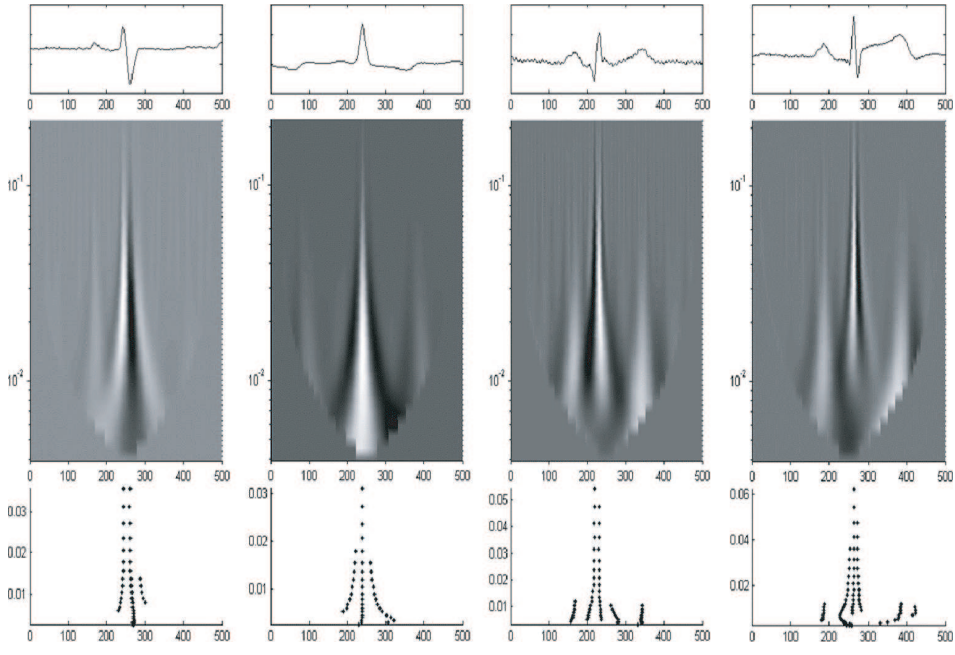

Fig. 2. Frequency analysis of four different QRS complexes using the Mexican hat-based CWT. The modulus maxima points plotted are those above a threshold of 90% from the overall maxima. Maxima and minima on the lower plot are indicated by bright white and dark black respectively.

These signals all show an ECG signal that demonstrates sinus rhythm. The characteristic waveform of sinus rhythm is produced when the electrical flow through the heart originates in the sino-atrial node in the right atrium, passes across the atrium and through the atrio-ventricular node and is then propagated evenly throughout the heart muscle (or myocardium) of the ventricles by the bundles of His. The P-wave of the ECG is produced when the atrium depolarises, the QRS complex corresponds to the depolarisation of the ventricles, and the T-wave represents the repolarisation of the ventricles.

It can be seen from Fig. 2, that the time-frequency distribution of energy depends on the morphology of the QRS signal. In the figure the maximum energies peak within the range 8–18 Hz. The energy of the first QRS peak is at about 12 Hz in the time frequency plane, the second broad single-humped QRS peaks at about 8 Hz, the third at 13 Hz, whereas the energy of the fourth complex peaks at about 18 Hz. The lower plots in Fig. 2 contain the *dominant* modulus maxima lines from the scalograms. These have been obtained by removing the modulus maxima lines, and parts thereof, that are below a threshold of the 90% of the value of the overall maximum value (i.e. the maxima of the maxima). P and T waves have their energy concentrated in low bands below 8 Hz. These lie below the frequency of the QRS wave.

In this study, for the wavelet-based detection of R waves we chose an energy range between 15 and 18 Hz, enabling us to separate out the QRS wave from the P and T waves (although the R waves may peak earlier, at 15–18 Hz they are always the most dominant maxima).

Figures 3 and 4 attempt to demonstrate the use of the modulus maxima by showing a CWT of a 3-second segment of ECG signal and the corresponding modulus maxima lines. Figure 3 shows the CWT of the signal using the Mexican hat based CWT, and Fig. 4 shows the modulus maxima lines of the same signal.

Each component of a single ECG complex has a different frequency representation that corresponds with a modulus maxima line of a different shape. QRS complexes have more energy and higher amplitude modulus maxima lines over a longer frequency interval, whilst P and T waves have less energy and lower amplitude modulus maxima lines over a shorter frequency interval. The QRS components also have a different shape to the rest of the ECG waveform, a difference that enables simple QRS detection. Modulus maxima lines therefore act as a summary of the useful information in the CWT of the signal.[26]

Figures 5 to 11 show ECG signals demonstrating different types of cardiac waveforms (i.e. ventricular tachycardia, bigeminy and ventricular fibrillation) analysed using the Mexican hat CWT. In all of them, the QRS complex has a wider frequency shape in comparison with the other waveform components (i.e. P or T waves). In all the figures, four different views of the modulus maxima lines are presented. The first view is a time-frequency diagram. The second view is a time-amplitude diagram. The third view is a frequency-amplitude diagram and the forth view is a 3D time-frequency-amplitude diagram. In these figures for clarity, low amplitude

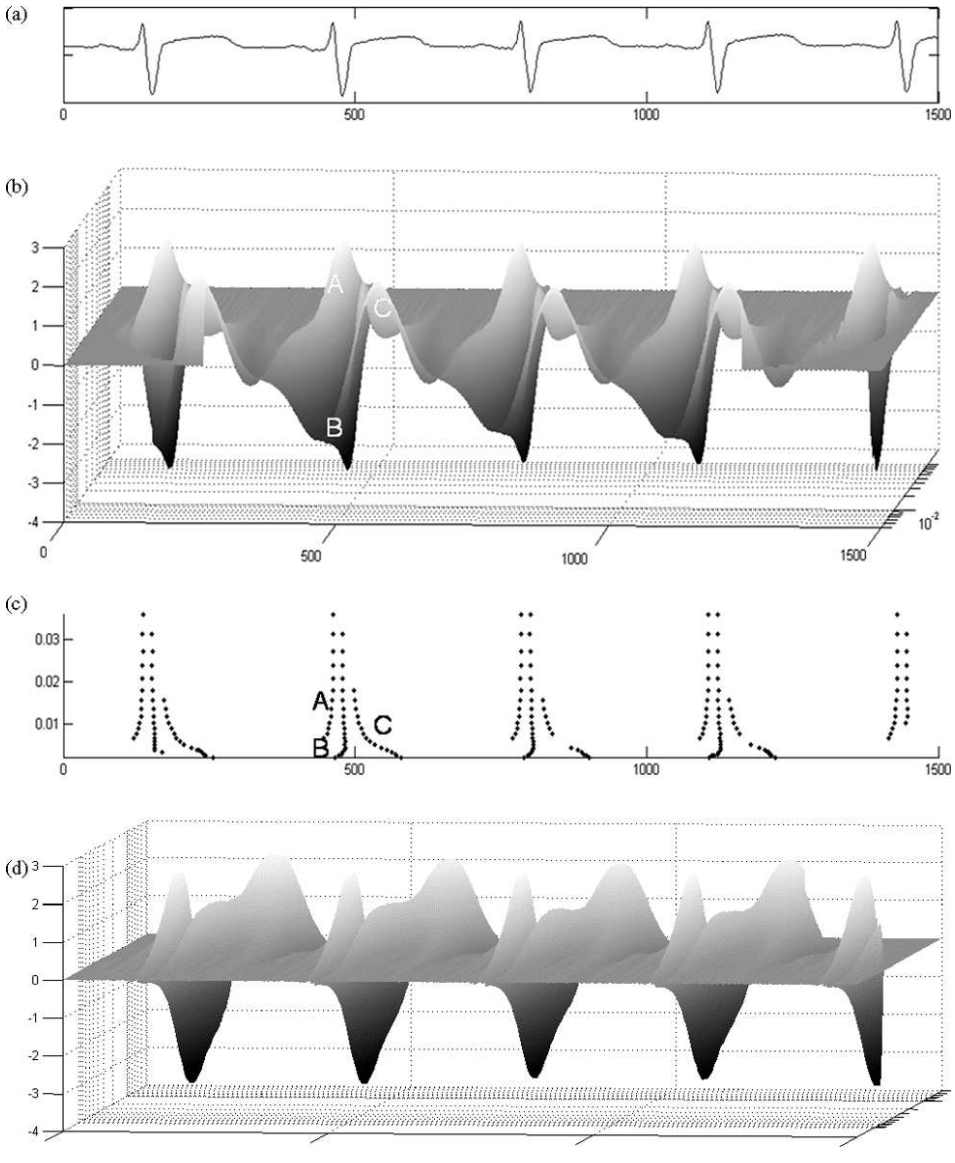

Fig. 3. Continuous Wavelet Transform of a 3.0-second signal, using the Mexican hat CWT. (a) Original ECG signal; (b) 3D view of the CWT; (c) modulus maxima points above a threshold of 90% from the overall maxima; (d) other 3D view of the CWT with the high frequencies at the front.

modulus maxima lines have been removed — those lines with amplitudes below 10% of the maxima overall have been ignored.

Figure 5 shows the analysis of a 1.0 second segment of ECG signal. Figure 5(a) shows a normal QRS complex, with a small Q-wave and an R and S wave of similar sizes. The T-wave is inverted (due to ischemia or infarction of the myocardium).

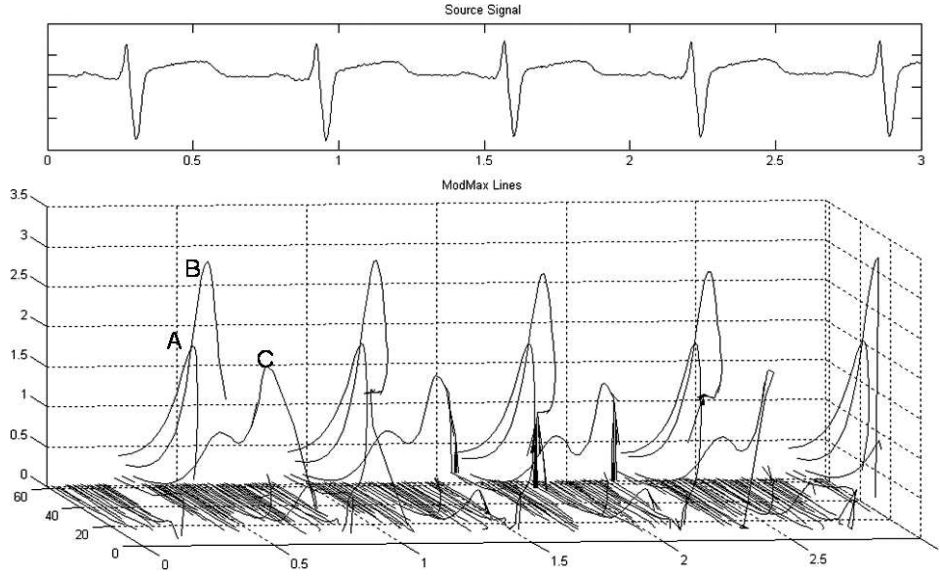

Fig. 4. Modulus maxima lines of a 5.0-second ECG signal using the Mexican hat CWT.

Four views of the corresponding modulus maxima are shown. All the components of the ECG waveform can be seen in the modulus maxima diagrams. Figure 5(b) to (e) show four views of the modulus maxima: plan view, end view in time, end view in frequency and a 3-D view. We can see from Fig. 5(e) that the maxima lines corresponding to the QRS are of high amplitude over a wide range of frequencies with frequency peaks at around 20 Hz. The maxima line corresponding to the P-wave is narrow, of a small amplitude, and has a frequency peak below 5 Hz. The maxima line corresponding to the T-wave has a high peak amplitude, almost the height of the R and S waves, but has a much sharper frequency curve peaking at around 7 Hz.

Figure 6 shows analysis of a 1.0 second ECG signal exhibiting ventricular tachycardia (VT). This occurs when the one part of the ventricle myocardium escapes from the normal electrical control of the heart, and the ventricles beat rapidly, but in a coordinated manner. There are modulus maxima lines corresponding to every maxima and minima of the VT waveform. These lines are of similar amplitude with the frequency concentrated below the 10 Hz, and the frequency peak at 5 Hz. No P or T wave can be seen in this example. This is because VT is an abnormal cardiac rhythm and its waveform does not possess characteristics normally associated with a normal cardiac (sinus) rhythm. Atrial electrical activity (if still occurring) is masked by the action of the ventricles, which have escaped from normal electrical control.

Figure 7 shows a bigeminy ECG waveform. This occurs when a normal beat originating from the sinus node alternates with an ectopic beat, that originates

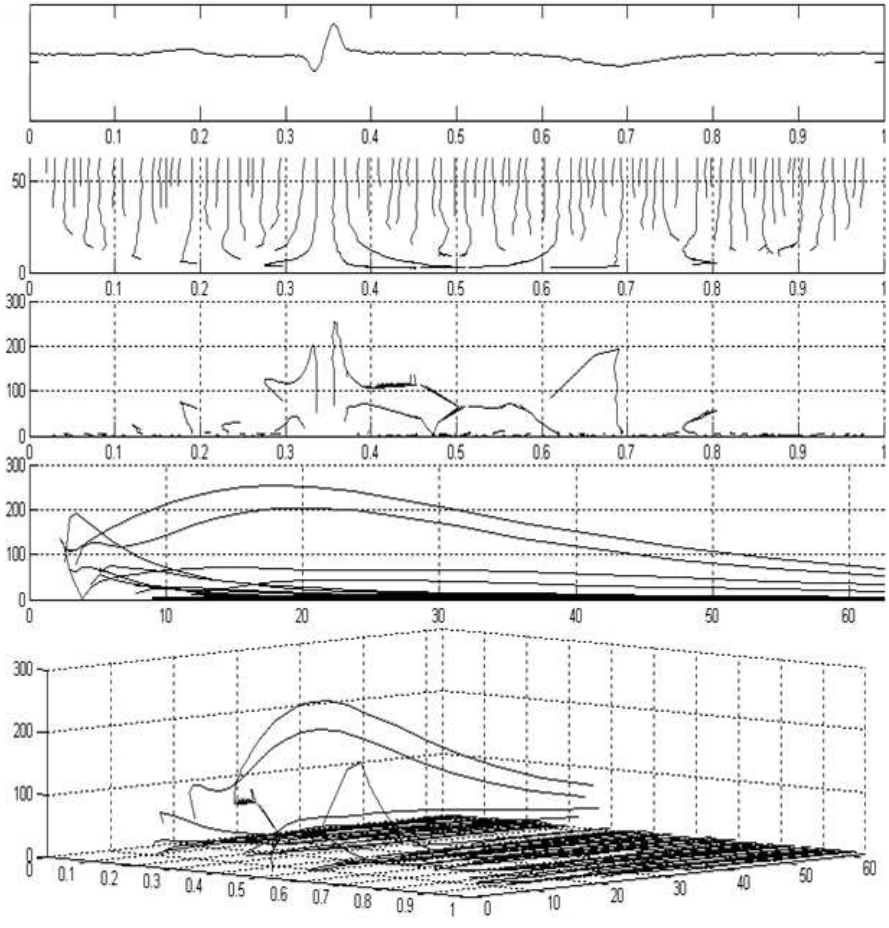

Fig. 5. Four views of modulus maxima lines of a 1.0-second ECG signal using the Mexican hat CWT. (a) The ECG signal; (b) plan view of the modulus maxima; (c) time-amplitude view of the modulus maxima; (d) frequency-amplitude view of the modulus maxima; (e) 3-D view of the modulus maxima.

early from somewhere in the ventricles. The 1.5-second sequence shows two QRS complexes with very different shapes. The first one is a sinus node generated QRS complex with a positive R-wave of high amplitude, the second complex is ectopic in origin, that is it originates from a part of the ventricle rather than part of the normal conducting pathway of the heart. The modulus maxima lines are wide in frequency for both cases, with peak frequencies at 10 Hz. The second beat has a large T-wave which produces a high amplitude modulus maxima line but with a more concentrated energy spectrum and a peak frequency at 2 or 3 Hz. This example shows that even with very different QRS complex morphologies, the QRS energy is more distributed in frequency than with the T-wave. Above 10 Hz, only the QRS modulus maxima lines have a considerable energy level.

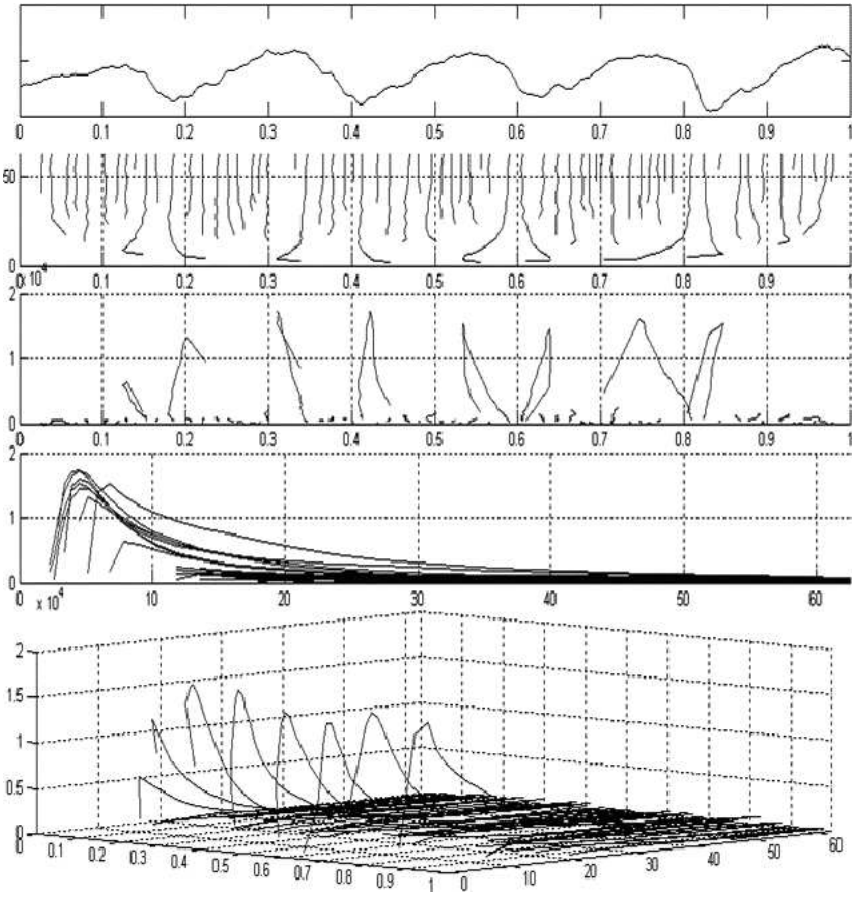

Fig. 6. Four views of modulus maxima lines of a 1.0-second ventricular tachycardia signal (legend as Fig. 5).

Figure 8 shows a normal sinus rhythm complex with a normal P, QRS and T-wave. All are clear, with normal amplitudes. In the modulus maxima space, the QRS complex has a wide shape with a frequency peak at 11 Hz, however the T-wave has a high amplitude line with a narrow shape, and a frequency peak at 3 Hz. Above 10 Hz the T-wave has lost almost all its energy. The P-wave produces a low amplitude modulus maxima line with a peak at 2 Hz.

Figures 9 to 11 show a sequence of three ECGs, each of 1.0-second duration taken before, during and after a ventricular fibrillation (VF) episode from a patient who presented with an inferior myocardial infarction at the Royal Infirmary of Edinburgh. VF is the primary cardiac arrhythmia associated with sudden cardiac death.[4] In VF, the ventricles again escape from the normal electrical control of the heart, however electrical activity originates from all parts of the ventricular myocardium in an uncontrolled manner. Many authors have attempted to shed light on the nature of the VF signal which is known to correlate to some

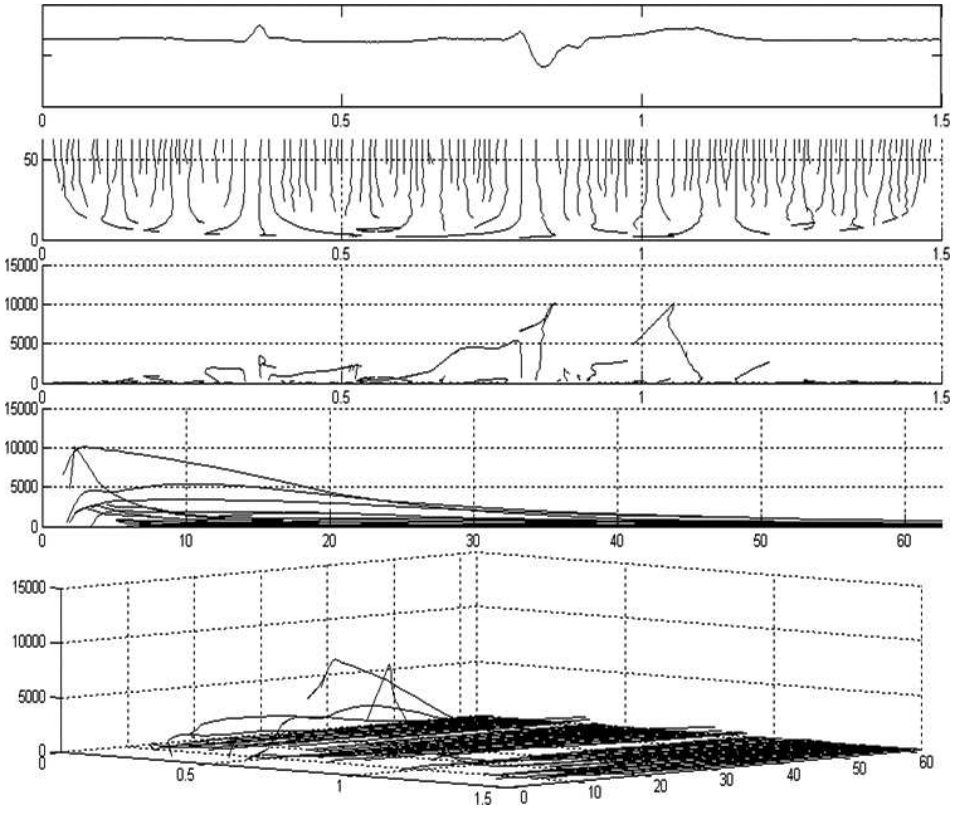

Fig. 7. Four views of modulus maxima lines of a 1.5-second bigeminy signal (legend as Fig. 5).

extent with the likelihood of survival from a defibrillation shock.[29] Figure 9 shows 1.0 second before the VF episode. The region of signal between the S and T point, the *ST segment*, is elevated (indicating cardiac ischemia or infarction). As in the previous examples, the P-wave does not produce a significant modulus maxima line, however both QRS and T waves generate high amplitude lines. While the T-wave has a high amplitude line and is concentrated in frequency with a peak at 2 or 3 Hz, the QRS complex has a wide frequency line with a peak at 12 Hz.

The VF signal (Fig. 10) has an irregular temporal morphology, which produces irregular modulus maxima lines in the frequency domain. In spite of this, some order can be seen in the modulus maxima lines which exhibit frequency peaks between 5 and 10 Hz. Figure 11 shows a 1.0 second signal just after the termination of VF. There is no P-wave visible. QRS and T waves are similar to Fig. 9. QRS complex generates modulus maxima lines wide in frequency and with a peak at 12 Hz. The T-wave is concentrated in frequency with a peak at 3 Hz.

Figure 12 contains the properly scaled ECGs corresponding to those analysed in Figs. 5 to 11. The traces considered in this section show that QRS modulus maxima

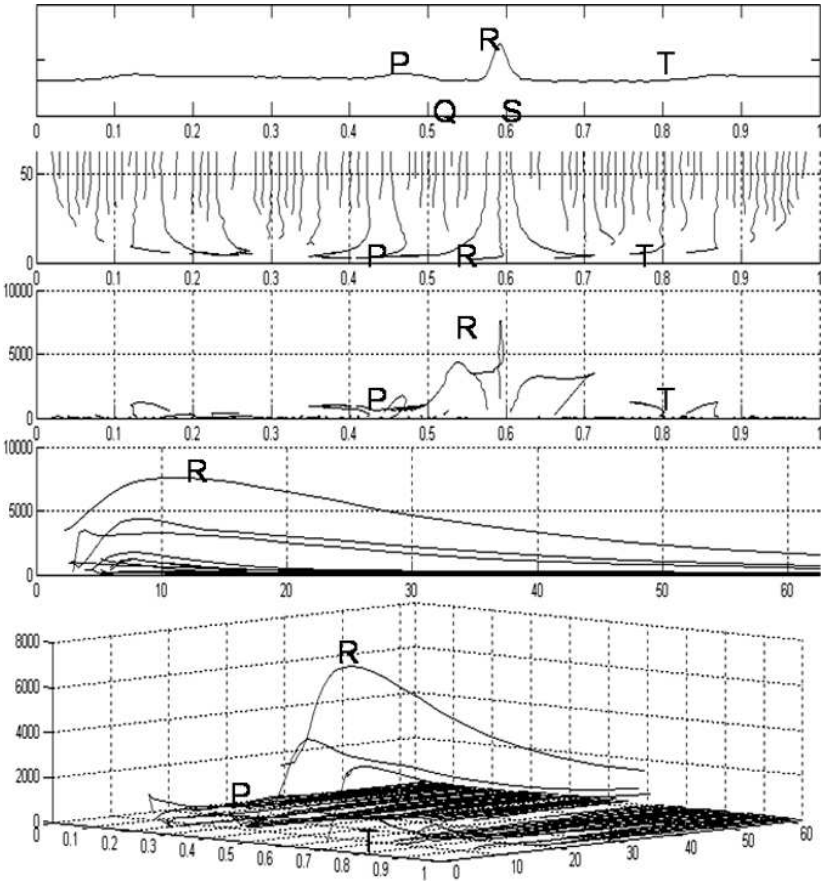

Fig. 8. Four views of modulus maxima lines of a 1.0-second signal of normal sinus rhythm. A clear R-wave and low voltage P and T waves can be seen (legend as Fig. 5).

lines have high amplitude over a wide frequency interval. The Mexican hat CWT produces three modulus maxima for the peak of the R-wave. This is shown clearly on the frequency-amplitude views. The T-wave also has a high amplitude maxima line, however, its peak is centred at lower frequencies. In this way, QRS complexes may be differentiated from other ECG features and used in a beat detection algorithm. This is the basis of the work described below.

4. A New Beat Detector Algorithm Based on Continuous Modulus Maxima

The QRS complex is the part of the ECG signal that displays the greatest deflection from the baseline. It represents the electrical depolarisation of the ventricles, which is followed by their contraction. On the standard ECG, a positive deflection from the baseline represents electrical activity going towards the ECG lead. The initial

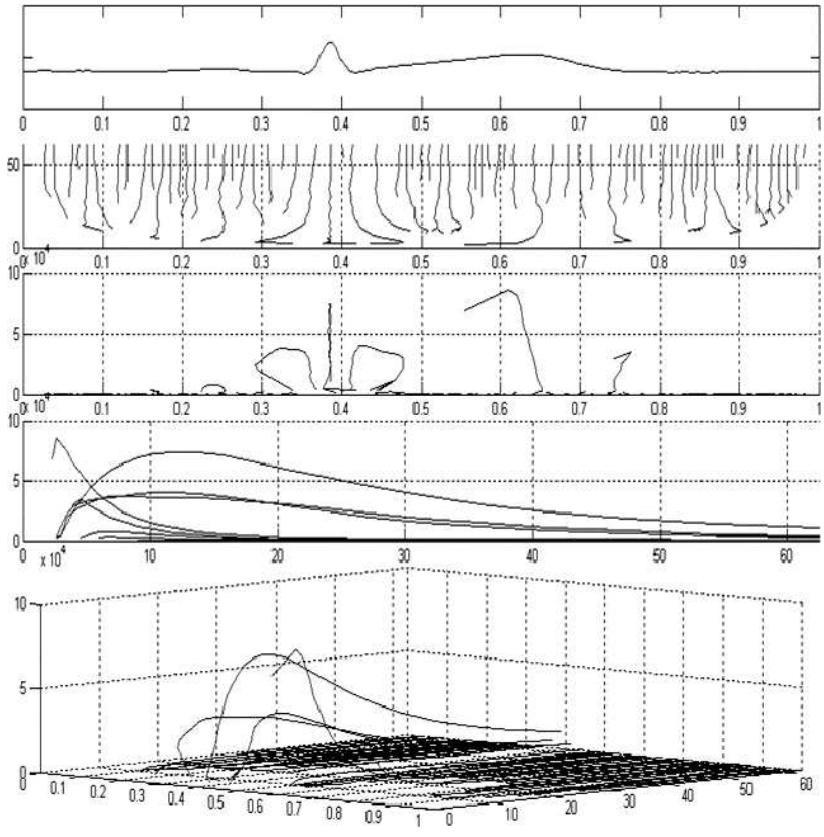

Fig. 9. Four views of modulus maxima lines of a 1.0-second signal just before an episode of VF (legend as Fig. 5).

downward deflection (if present) at the start of the QRS complex is termed the "Q" wave and the following upwards deflection is termed the "R" wave. The final part of the QRS complex is the next downward deflection, which is termed the "S" wave. Sometimes there may be no initial downward deflection (Q wave) and a second upwards deflection at the end of the QRS is present, a second "R" wave.

In a normal heart, the size of the initial downward "Q" deflection and relative size of the subsequent upward "R" deflection depends on which of the normal 12 leads are being considered, and also on underlying pathology. The QRS complex in the chest leads shows a steady progression from V1, where it is predominantly downwards (no Q-wave, large R-wave), to V6 where it is predominantly upwards. The point where the R-wave and S-wave are of equal sizes is termed the "transition point" and represents the site of the ventricular septum, the muscle wall in between the left and right ventricular walls.

The R-wave detector is an extremely useful tool for the analysis of the ECG signal. It is used both for finding the fiducial points employed in ensemble averaging

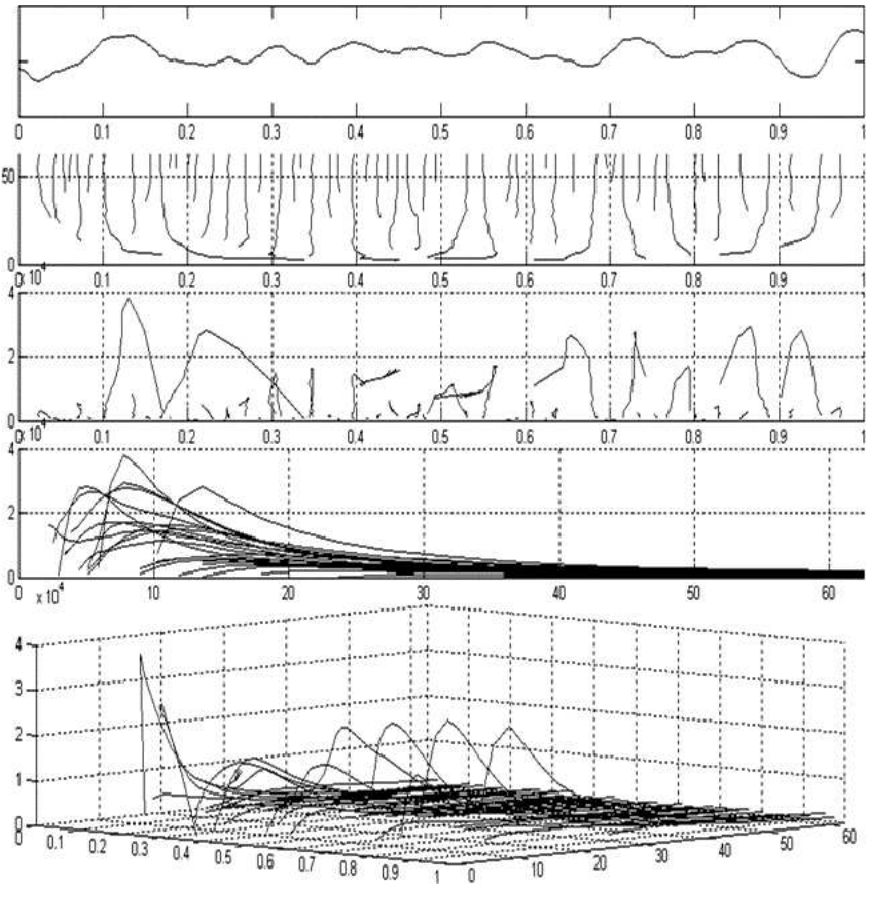

Fig. 10. Four views of modulus maxima lines of a 1.0-second signal during a VF episode (legend as Fig. 5).

analysis methods, and for computing the R–R time series from which a variety of heart rate variability (HRV) measures can be derived, e.g. SDNN and NN50 etc.[28] Both these techniques rely on the accurate determination of the temporal location of the R-wave. There are currently a number of QRS detection algorithms available which use a variety of signal analysis methods. The most common of these are based on signal matched filters or time-frequency decomposition methods.

Other less common methods have also been proposed including neural networks, genetic algorithms and syntactic methods (Köhler *et al.*[6] have performed an analysis of the most important QRS complex detectors currently available). Recently, wavelet-based QRS detection methods have been suggested by a number of groups. These include Li *et al.*[7] who proposed a method based on finding the modulus maxima larger than a threshold obtained from the pre-processing of some initial beats. In Li *et al.*'s method, the threshold is updated during the analysis to obtain a better performance. This method has a post-processing phase in which redundant

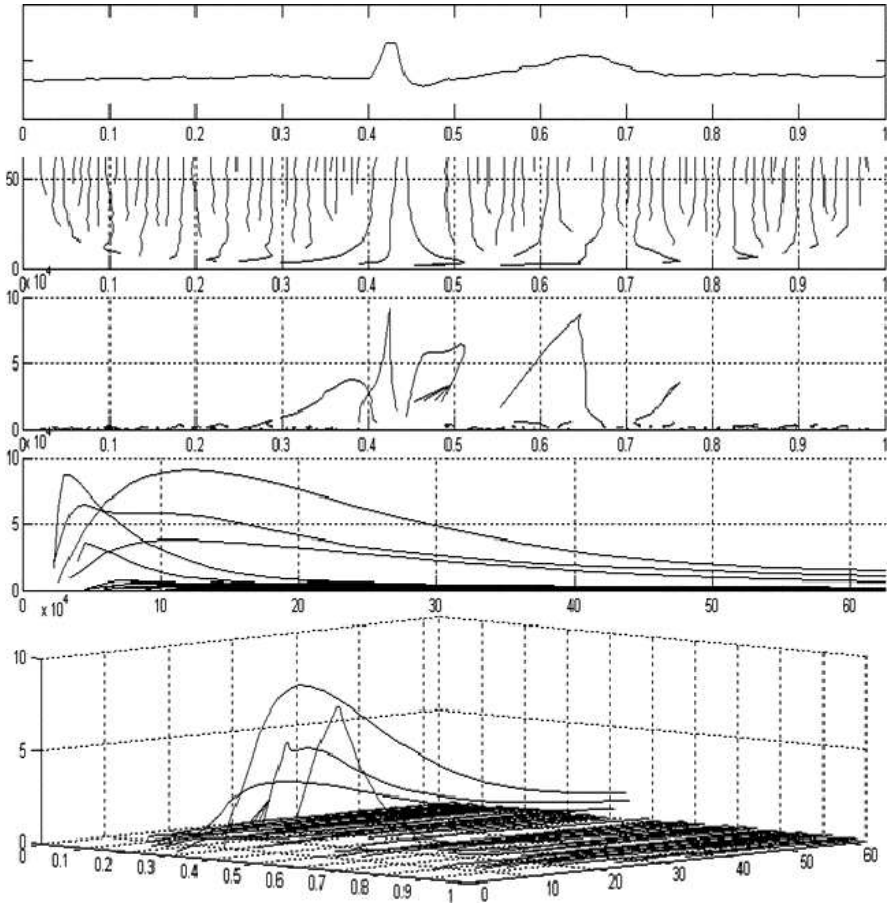

Fig. 11. Four views of modulus maxima lines of a 1.0-second ECG signal just after an episode of VF (legend as in Fig. 5).

R waves or noise peaks are removed. A last stage is necessary where the R peak is found. The algorithm achieves a good performance with a sensitivity of 99.90% and positive prediction value of 99.94% when tested on the MIT/BIH database. However, the use of further stages for the removal of false R waves due to noise or redundancy, although increasing its performance, also complicates the algorithm. Li *et al.* also describe a method for finding other characteristic points within the ECG once the R-wave has been found, including the QRS onset and offset and the P and T waves. Kadambe *et al.*[8] have described an algorithm which finds the local maxima of two consecutive Dyadic Wavelet scales, and compares them to classify local maxima produced by R waves and by noise. This method, based on the Dyadic Wavelet Transform, obtains a sensitivity of 96.84% and a positive predictive value of 95.20% when tested on four 30-minute tapes acquired from the American Heart Association (AHA) database. The features and performance of the algorithms of

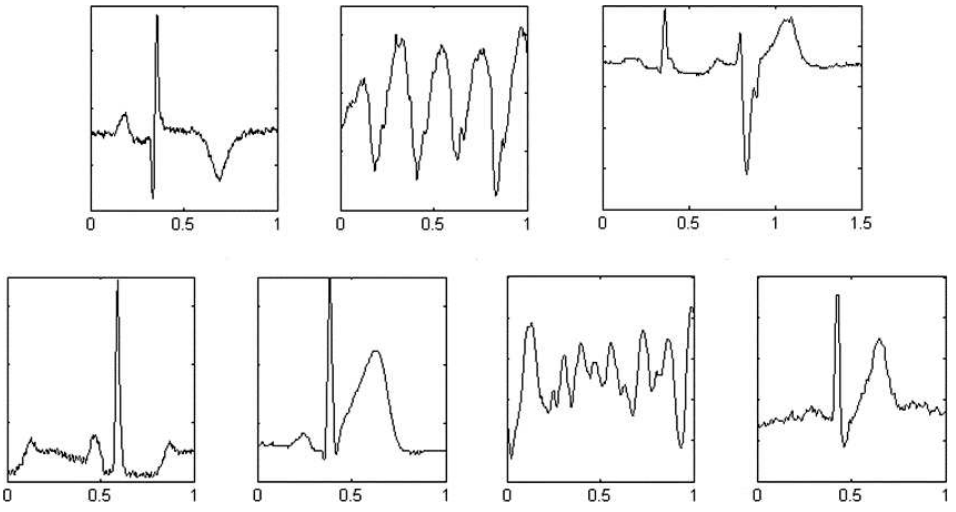

Fig. 12. Real time representations of Figs. 5 to 11.

Li *et al.* and Kadambe *et al.* are considered further, in the context of the current work, in the concluding section of this paper.

We present here an improved method for R-wave detection based on Continuous Wavelet Transform Modulus Maxima. The use of continuous maxima lines allows, rather than discrete or dyadic maxima allows the maxima associated with the R-wave to be followed much more accurately across frequencies in the time-frequency plane. This is because in our CWT-based method we can achieve arbitrarily high frequency resolution in the time-frequency plane, (i.e. there is no dyadic frequency jump as is associated with the dyadic wavelet transform) and hence maxima can be better resolved and hence followed. This is particularly important when there is significant noise in the signal which can result in a multitude of maxima appearing towards the high frequency region of the time-frequency plane.

Our method is simple and robust, does not involve excessive computation and offers a good performance with sensitivity and positive predictive values similar to the highest performance algorithms currently available.[6] These key features make it suitable for small devices that require algorithms with low computational costs. In addition, the algorithm does not require pre-filtering and is robust against interference signals such as EMG noise or movement artefact. It is also worth noting that our technique may be employed in the detection of other features within the ECG, such as P and T waves.

Using the properties of the modulus maxima illustrated in the previous section, a new R-wave detector is proposed. The algorithm is described as follows in conjunction with the schematic diagram shown in Fig. 13:

(1) The CWT is computed within a selected frequency interval. As explained in Sec. 5 the best performance was obtained in the frequency interval 15–18 Hz.

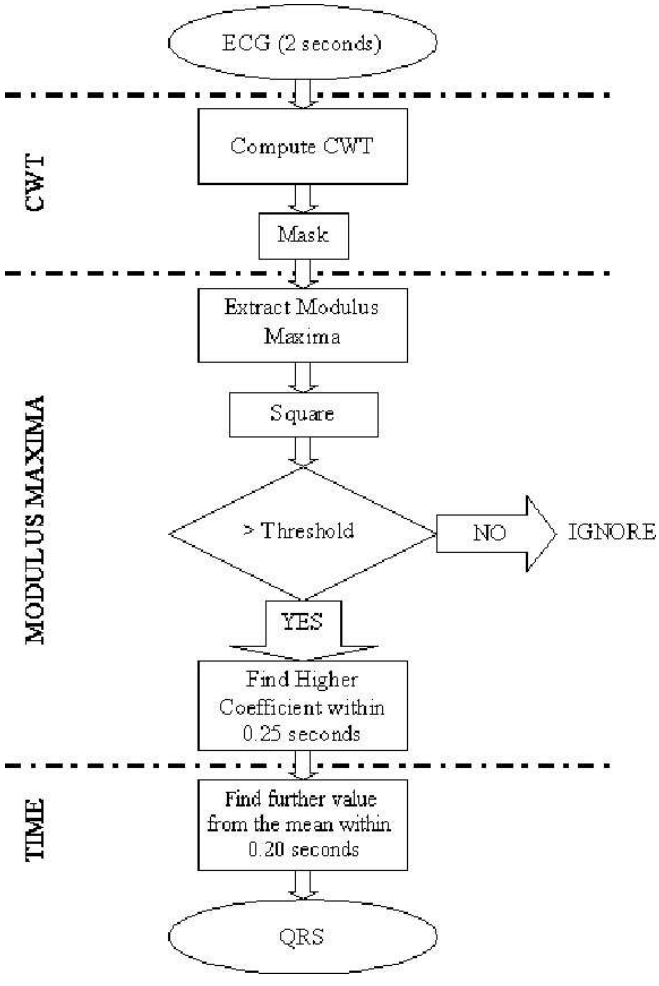

Fig. 13. Schematic diagram of the beat detection algorithm.

A mask is applied to remove edge effects. This mask is set to four times the a scale of the wavelet which we have found through trial and error, provides optimal removal of edge components.

(2) The modulus maxima of the CWT are extracted. The square of the modulus is taken, as it emphasizes the difference between coefficients. Maxima lines below the preset threshold are ignored. We chose a universal preset threshold corresponding to a fixed percentage of the maximum value of the modulus maxima coefficients. As shown later the best performance was obtained for a threshold of 30%.

(3) The remaining modulus maxima are taken as possible R-wave points. All modulus maxima found within an interval of 0.25 seconds of each other are then inspected in turn and the point with the maximum coefficient value is selected

as the R-wave point. We assume that all the coefficients within this interval of 0.25 seconds over the threshold are due the same QRS complex so we only consider one of them.

(4) Once the R-wave points are selected, we turn back to the time domain to find the exact location of the R-wave. We calculate the mean value of 0.10 seconds before and after the points detected in the Modulus Maxima Domain. Then we locate the point within the same interval of 0.20 seconds where the signal is furthest from the mean. This step is necessary because in the frequency interval we employ, the Modulus Maxima line does not necessarily point to the exact location in time of the R-wave peak.

The algorithm described above is applied within a 2-second window along the signal. We have found that longer segments may contain a QRS with large amplitude which results in a high threshold being set, hence lower voltage QRS complexes within the same segment may fall below this threshold and be ignored.

Examples of the R-wave detection algorithm are shown in Fig. 14 for a variety of ECGs exhibiting normal sinus rhythm of differing morphologies, arrhythmias and

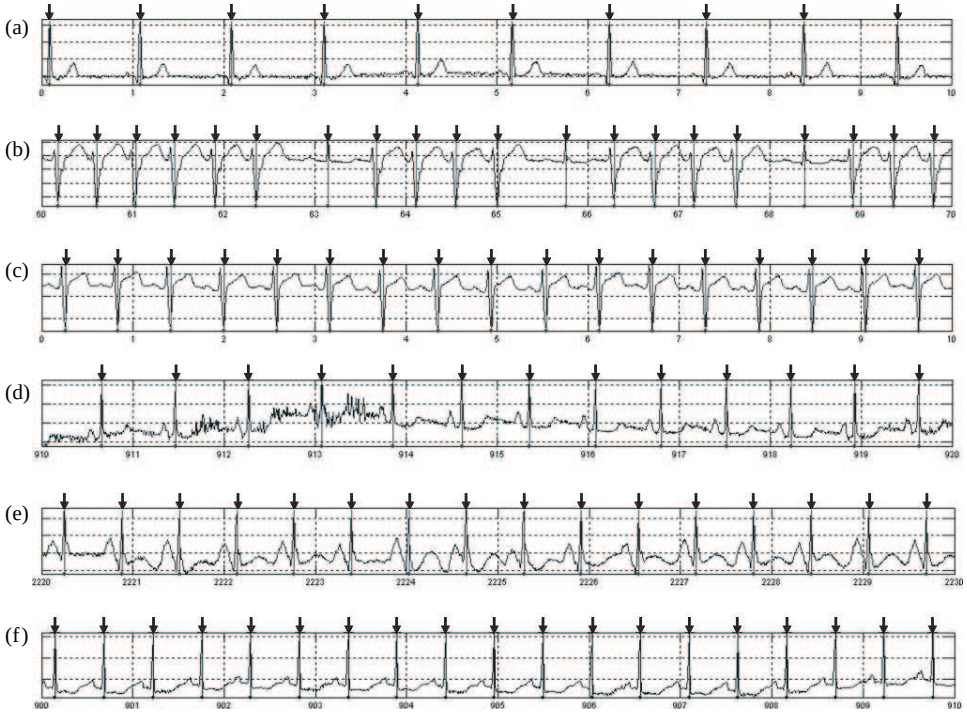

Fig. 14. Examples of the wave detection algorithm. (a) ECG with very clear QRS complexes. (b) ECG with QRS complexes with very different morphologies. (c) ECG with a QRS complex with a big S-wave. (d) ECG with some noise. (e) ECG with noise and high P-wave. (f) ECG with clear QRS complexes and small P-wave.

ectopic QRS complexes. The vertical black arrows shown in the plots denote the location of the detected R waves. Both positive (14a, 14d, 14e, 14f) and negative (14b, 14c) QRS complexes were analysed. In addition, Fig. 14(d) demonstrates that the algorithm can cope with significant signal noise. The algorithm was tested using two comprehensive databases to determine optimum values for the frequency range and threshold value. Results from this testing are given in the following section.

5. Results from the Testing of the New Algorithm

The new R-wave detection algorithm was tested against two datasets. These were the MIT/BIH database and our own in-house ECG database.

5.1. *Validation with MIT/BIH database*

The new R-wave detection algorithm was first tested with the MIT database as a standard reference. The MIT/BIH is a standard database used for performance comparisons with other algorithms. Our algorithm was tested with the most common MIT/BIH signals. The MIT/BIH signals used in the study are given in the left column of Table 1. To analyse the best performance, different range of scales

Table 1. Results of the QRS detector algorithm with the MIT/BIH database.

Sign	Th (%)	Scales	Beats	TP	FP	FN	Se	P+
100	30	[5-6]	2270	2270	0	0	100	100
101	30	[5-6]	1864	1863	5	1	99.95	99.73
102	30	[5-6]	2185	2185	0	0	100	100
103	30	[5-6]	2082	2082	0	0	100	100
104	30	[5-6]	2227	2213	29	14	99.37	98.71
105	30	[5-6]	2570	2557	63	13	99.49	97.6
106	30	[5-6]	2026	2025	0	1	99.95	100
107	30	[5-6]	2135	2132	1	3	99.86	99.95
118	30	[5-6]	2277	2277	1	0	100	99.96
119	30	[5-6]	1985	1985	0	0	100	100
200	30	[5-6]	2599	2596	5	3	99.88	99.81
201	30	[5-6]	1962	1912	1	50	97.45	99.95
202	30	[5-6]	2134	2129	0	5	99.77	100
203	30	[5-6]	2978	2943	51	35	98.82	98.3
205	30	[5-6]	2654	2651	0	3	99.89	100
208	30	[5-6]	2953	2926	13	27	99.09	99.56
209	30	[5-6]	3003	3003	6	0	100	99.8
210	30	[5-6]	2647	2633	4	14	99.47	99.85
212	30	[5-6]	2746	2746	1	0	100	99.96
213	30	[5-6]	3248	3245	0	3	99.91	100
214	30	[5-6]	2259	2256	2	3	99.87	99.91
215	30	[5-6]	3360	3359	1	1	99.97	99.97
217	30	[5-6]	2207	2206	3	1	99.95	99.86
219	30	[5-6]	2152	2152	0	0	100	100
Total			58523	58346	186	177	99.7	99.68

and different threshold values were tested. An initial set of frequency ranges were examined. These were: 90–18 Hz, 18–9 Hz, 9–6 Hz, 6–4.5 Hz, 4.5–3.6 Hz, 3.6–3 Hz, 3–2.57 Hz and 2.57–2.25 Hz. For each signal and frequency range, the following thresholds were tested: 10%, 20%, 30%, 40%, 50%, 60%, 70%, 80% and 90%.

The best performance was obtained using the range 90–18 Hz and a threshold of 30%. In order to refine the performance of the algorithm, a second set of tests were preformed using the threshold of 30% and the frequency intervals of 90–30 Hz, 30–18 Hz, 22.5–18 Hz, 18–15 Hz and 15–12.86 Hz.

The best overall performance was achieved using the frequency range 18–15 Hz. This resulted in a sensitivity of 99.7% and a positive predictivity of 99.68% for the MIT/BIH database. The frequency range 18–15 Hz corresponds to only two scales: $a = 5$ and 6. Thus the algorithm requires only the transformation of these signals at these two scales, thus in practice providing quick implementation.

The complete results are given in Table 1. MIT signals have a sampling frequency of 360 Hz and we employed the Mexican hat wavelet as the mother wavelet in our algorithm. Using Eq. (9) (Sec. 2) the scales corresponding to each frequency level is determined. The algorithm was implemented using MatLab version 6.0 running on a Pentium IV computer with 1.6 GHz of clock speed. Each signal of the MIT database contains approximately half an hour of ECG data. The calculation time for each MIT signal was around 25 seconds.

5.2. *Validation with continuous CCU data*

Our group has installed equipment within the Coronary Care Unit (CCU) at the Royal Infirmary of Edinburgh to collect ECG signals continuously from all five beds within the unit (for more details see Refs. 27 and 30). Protocols were formulated for data collection and archiving of the collected signals. Data collected was archived over a one-year period (requiring approximately 3 GB of storage per week for a signal sample rate of 500 Hz). The technology is now available to perform this task in a compact, easily accessible form at a reasonably affordable price. Archiving the whole ECG time series for each patient allows an analysis of the signal using a variety of techniques. The main aim of the data collection was to obtain patient signals when the patient went into VF. The complete data set is also available to be revisited in the future, when further analysis can be done on other parts of the ECG dataset.

Our algorithm was tested with ten 1-hour signals exhibiting normal sinus rhythm taken at random from the complete database. The signals were extremely heterogeneous, with many containing a large number of ectopic beats and arrhythmic events, and some exhibiting considerable noise (Fig. 14). As can be seen from Table 2, there were 132 false positives and 231 false negatives over the 48495 collected beats. This gave a sensitivity of 99.53% and a positive predictivity of 99.73%. A breakdown of the results for each signal is provided in Table 2.

Table 2. Results of the QRS detector algorithm with the Edinburgh CCU data.

Signal	True positives	False positives	False negatives
B5_23Sep02_h12.bin	5491	13	7
B1_14Sep02_h12.bin	5202	7	16
B5_25Aug02_h12.bin	4148	25	93
B1_11Oct02_h12.bin	5249	9	8
B3_13Oct02_h12.bin	4361	6	0
B2_16Jul02_h12.bin	4126	0	34
B2_06Jul02_h12.bin	5089	8	9
B5_06Jun02_h12.bin	4694	0	0
B5_15May02_h13.bin	4632	63	23
B5_13Apr02_h12.bin	5503	1	41
Total	48495	132	231

6. Conclusions

We have applied continuous wavelet transform modulus maxima methods to the problem of ECG signal characterisation and specifically R-wave identification. We have provided a pictorial library of the CWTMM associated with the ECGs from both diseased and healthy hearts. An algorithm for the robust detection of R-waves was then detailed together with the results from its application to two rhythm databases. The R-wave detector algorithm gave exemplary results for both the *in-house* database and the "standard" MIT/BIH databases. We showed that continuous modulus maxima techniques offer very good accuracy in QRS detection. The algorithm proposed offers a sensitivity of 99.53% and a positive predictivity of 99.73% with our own signals obtained from the Coronary Care Unit at the Royal Infirmary of Edinburgh, and a sensitivity of 99.7% and a positive predictivity of 99.68% with the standard MIT/BIH database signals. Our method simplifies the technique of QRS detection using wavelets, but maintains a level of functioning (with rates over 99.5%) on par with the best algorithms proposed in the literature.[6] The computation time is not high because it uses an efficient frequency interval, which contains the most significant part of the spectral energy distribution. Preprocessing is not required as the method is robust against the noise or interference signals produced by muscle activity (electromyograms) and breathing.

Li *et al.*[7] proposed algorithm also applied a modulus maxima-based technique to the detection of R waves. Their methods involved four steps:

(1) Search for modulus maxima lines that correspond to R waves in the Frequency Range: 4–125 Hz (over four discrete wavelet scales).
(2) Calculate the singular degree to eliminate those modulus maxima lines corresponding to noise or interferences.
(3) Eliminate isolation and redundant modulus maxima lines.
(4) Detect the R-peak.

This algorithm uses four different thresholds, one for each scale, which is variable and requires updating during the detection process. The algorithm achieves a very good performance, with a sensitivity and specificity very similar to our own, however, the use of several algorithmic post processing stages complicates the algorithm. Our proposed algorithm does not have this additional complexity associated with it, hence improving the speed of computation and reducing energy consumption necessary for implementation within a mobile medical device.

Kadambe *et al.*[8] proposed algorithm using the Dyadic Wavelet Transform (DyWT) instead of the Continuous Wavelet Transform employs a fixed threshold to detect the peaks of the Wavelet Transform. The algorithm is simple and achieves a good performance on the limited data they tested it with (AHA database). However, the Dyadic Wavelet Transform employs discrete jumps in frequency levels in the transform space. The CWT-based algorithm we employ affords high frequency resolution and therefore allows a better definition of the QRS maxima curves. This allows them to be followed across scales in noisy signals and better defines the spectral region corresponding to the QRS maxima peak.

As stated above the main requirement of the current methodology is for beat detection, hence the exact location of the R-wave is not the main consideration. However for some ECG analyses, knowledge of the exact location of the R-wave may be desirable (e.g. for the detection of ventricular late potentials). Should this be a requirement, the current proposed method may be refined to more accurately determine the precise temporal location of the R-wave peak point.

Modulus maxima lines follow a wandering path across frequency scales determined by the morphology associated with the ECG signal features. Hence, the algorithm as described in this paper, can for some sinus rhythm morphologies "locate" the R-wave at a point offset from the R-wave peak. This is not a problem either for subsequent temporal averaging methods or for HRV analysis as the offset remains constant from beat-to-beat. However, if the exact temporal location of the R-wave peak is required, two possible methods may be used. The first method for finding the R-wave peak is to follow the modulus maxima line up the highest frequencies. This method however, is problematic as algorithms that track the modulus maxima line often confuse the high frequency noise maxima with the high frequency part of the R-wave maxima line, due to their close temporal separation. A second more robust method, is to use the modulus maxima lines to determine the temporal location of the QRS complex then flips back into the time domain to follow the R-wave ECG signal towards its peak. We are currently working on this latter method.

References

1. I. Romero Legarreta, L. Serrano and U. Ayesta, ECG frequency domain features extraction: A new characteristic for arrhythmias classification, in *29th Annual Int. Conf. of the IEEE Engineering in Medicine and Biology Society*, Istanbul, Turkey, 25–28 October 2001.

2. U. Ayesta, L. Serrano and I. Romero Legarreta, Complexity measure revisited: A new algorithm for classifying cardiac arrhythmias, in *29th Annual Int. Conf. of the IEEE Engineering in Medicine and Biology Society*, Istanbul, Turkey, 25–28 October 2001.
3. P. S. Addison, J. N. Watson, G. Clegg, M. Holzmer, F. Sterz and C. Robertson, Evaluating arrhythmias in ECG signals using wavelet transforms, *IEEE Engrg. Med. Biol.* **19** (2000) 383–392.
4. P. S. Addison, J. N. Watson, G. Clegg, P. A. Steen and C. Robertson, Finding coordinated atrial activity during ventricular fibrillation using wavelet decomposition, *IEEE Engrg. Med. Biol.* **21** (2002) 58–65.
5. P. S. Addison, J. N. Watson, G. Clegg, M. Holzmer, F. Sterz and C. Robertson, A novel wavelet transform based analysis reveals hidden structure in ventricular fibrillation, *Resuscitation* **43** (2000) 121–127.
6. B. U. Köhler, C. Hennig and R. Orglmeister, The principles of software QRS detection, *IEEE Engrg. Med. Biol.* **21** (2002) 42–57.
7. C. Li, C. Zheng and C. Tai, Detection of ECG characteristic points using wavelet transforms, *IEEE Trans. Biomed. Engrg.* **42** (1995) 21–28.
8. S. Kadambe, R. Murray and G. F. Boudreaux-Bartels, Wavelet transform-based QRS complex detector, *IEEE Trans. Biomed. Engrg.* **46** (1999) 838–848.
9. W. Chen, M. D. Novak, T. A. Black and X. Lee, Coherent eddies and temperature structure functions for three contrasting surfaces. Part 1: Ramp model with finite microfront time, *Boundary-Layer Meteo.* **84** (1997) 99–123.
10. W. Gao and B. L. Li, Wavelet analysis of coherent structures at the atmosphere-forest interface, *J. Appl. Meteo.* **32** (1993) 1717–1725.
11. C.-H. Lu and D. R. Fitzjarrald, Seasonal and diurnal variations of coherent structures over a deciduous forest, *Boundary-Layer Meteo.* **69** (1994) 43–69.
12. I. Daubechies, *Ten Lectures on Wavelets*, CBMS-NSF Regional Conference Series in Applied Mathematics (SIAM, 1992).
13. R. R. Coifman and D. L. Donoho, Translation invariant de-noising, *Lect. Notes Statist.* **103** (1995) 125–150.
14. P. S. Addison, *The Illustrated Wavelet Transform Handbook: Applications in Science, Engineering, Medicine and Finance* (Inst. Phys. Publishing, 2002).
15. P. S. Addison, J. N. Watson and T. Feng, Low-oscillation complex wavelets, *J. Sound Vib.* **254** (2002) 733–762.
16. J. N. Watson, P. S. Addison, Spectral-temporal filtering of NDT data using wavelet transform modulus maxima, *Mech. Res. Commun.* **29** (2002) 99–106.
17. J. N. Watson, P. S. Addison, N. Grubb, G. Clegg, C. Robertson and K. A. A. Fox, Wavelet-based filtering for the clinical evaluation of atrial fibrillation, in *29th Annual Int. Conf. of the IEEE Engineering in Medicine and Biology Society*, Istanbul, Turkey, 25–28 October 2001.
18. S. Roux, J. F. Muzy and A. Arneodo, Detecting vorticity filaments using wavelet analysis: about the statistical contribution of vorticity filaments to intermittency in swirling turbulent flows, *Euro. Phys. J.* **B8** (1999) 301–322.
19. J. S. Sahambi, S. M. Tandon, R. K. P. Bhatt, Using wavelet transforms for ECG characterization: An on-line digital signal processing system, *IEEE Engrg. Med. Biol.* **16** (1997) 77–83.
20. J. S. Sahambi, S. M. Tandon and R. K. P. Bhatt, Quantitative analysis of errors due to power-line interference and base-line drift in detection of onsets and offsets in ECG using wavelets, *Med. Biol. Engrg. Comput.* **35** (1997) 747–751.
21. B.-L. Li and C. Loehle, Wavelet analysis of multiscale permeabilities in the subsurface, *Geophys. Res. Lett.* **22** (1995) 3123–3126.

22. L. M. Bruce and R. R. Adhami, Classifying mammographic mass shapes using the wavelet transform modulus-maxima method, *IEEE Trans. Med. Imag.* **18** (1999) 1170–1177.
23. R. A. Carmona, W. L. Hwang and R. D. Frostig, Wavelet analysis for brain-function imaging, *IEEE Trans. Med. Imag.* **14** (1995) 556–564.
24. M. Haase and B. Lehle, Tracing the skeleton of wavelet transform maxima lines for the characterisation of fractal distributions, *Fractals and Beyond*, ed. M. M. Novak (World Scientific, 1998).
25. M. E. Degaudenzi and C. M. Arizmedi, Wavelet-based fractal analysis of airborne pollen, *Phys. Rev.* **E59** (1999) 6569–6573.
26. S. Mallat, *A Wavelet Tour of Signal Processing*, 2nd edn. (Editorial Academic Press, 1999).
27. I. Romero Legarreta, J. N. Watson, P. S. Addison, N. Grubb, G. Clegg, C. Robertson and K. A. A. Fox, Time-frequency analysis of the ECG preceding ventricular fibrillation from a continuously collected CCU signal, *2nd European Medical and Biological Engineering Conference*, Vienna, Austria, 4–8 December 2002.
28. Task force of the European Society of Cardiology and the American Society of Pacing and Electrophysiology. Heart rate variability: Standards of measurement, physiological interpretation, and clinical use, *Circulation* **93** (1996) 1043–65.
29. M. J. Reed, G. R. Clegg and C. E. Robertson, Analysing the ventricular fibrillation waveform, *Resuscitation* **57** (2003) 11–20.
30. I. Romero Legarreta, M. Reed, J. N. Watson, P. S. Addison, N. Grubb, G. R. Clegg, C. E. Robertson and K. A. A. Fox, The long term continuous collection of high resolution ECG signals from a coronary care unit, in *Computers in Cardiology*, Thessaloniki, Greece, 21–24 September 2003.